Real-Time Charging Navigation of Electric Vehicles to Fast Charging Stations: A Hierarchical Game Approach

Article *in* IEEE Transactions on Smart Grid · August 2015

DOI: 10.1109/TSG.2015.2458863

CITATIONS
3

READS
93

2 authors, including:

Jun Tan
University of Wisconsin - Milwaukee
17 PUBLICATIONS **41** CITATIONS

SEE PROFILE

Real-Time Charging Navigation of Electric Vehicles to Fast Charging Stations: A Hierarchical Game Approach

Jun Tan, *Student Member, IEEE*, and Lingfeng Wang, *Member, IEEE*

***Abstract*—This paper proposes an integrated electric vehicle (EV) charging navigation framework, which takes into consideration the impacts from both the power system and transportation system. The proposed framework links the power system with transportation system through the charging navigation of massive EVs. It benefits the two systems by attracting EVs to charge at off-peak hours and saving the time of EV owners with real-time navigation. Based on the formulated framework, a hierarchical game approach is proposed in this paper to effectively navigate EVs to electric vehicle charging stations (EVCSs). At the upper level of the hierarchical game, a non-cooperative game is proposed to model the competition between EVCSs. Based on the pricing strategies obtained from the non-cooperative game, multiple evolutionary games are formulated at the lower level to evolve EVs' strategies in choosing EVCSs. The simulation results show that the proposed integrated charging navigation approach is effective in improving both the reliability of the power distribution grid and economic profits of the charging stations.**

***Index Terms*—Charging navigation, charging station, electric vehicle (EV), game theory, traffic flow.**

I. Introduction

WITH THE increasing penetration of electric vehicles (EVs) and the development of charging infrastructure, the electric vehicle charging stations (EVCSs) are becoming a vital recharging source for EVs. Home charging at house garages may be more convenient for the EV owners. For people living in urban areas with high population density, the accessibility of personal garages is limited and public charging stations are needed to recharge their EVs. Moreover, EVCSs can offer lower charging prices for EVs compared with home charging, as power can be purchased at a lower rate from the wholesale power market [1]. Also, EVCSs are a much needed recharging infrastructure for long-distance travelers who may run out of their batteries before returning home. These merits make the EVCS a promising charging infrastructure. However, as the penetration level of EVs grows, the intermittent charging loads may place additional stress on the power system by overloading the distribution transformers and transmission lines.

Various studies have been conducted for investigating EVs' impacts on the power system [1]–[12]. Most of them assumed that EVs are charged at home, which are focused on controlling the charging process of EVs in order to shave the peak load or improve the power quality [8]–[12]. For the charging station, the charging duration is much shorter than the home charging. With fast charging, EVs can be charged to full state of charge (SoC) within half an hour [1]–[3], while the home charging needs 6–8 h. Thus, mitigating the negative impact of EVs on power systems through controlling the charging duration and charging rate of EVs is not applicable for the scenario of charging stations. One promising solution is to attract EVs to charge at appropriate times so as to optimize the charging load of EVCSs. In this case, the impact from the transportation system is not negligible for the management and coordination of multiple EVCSs. Guo *et al.* [3] proposed a rapid charging navigation system for EVs based on the power system coupled with the traffic data accounting for the impact due to traffic flow. The power market is also a factor that should be considered in managing EVCSs. Multiple EVCSs in the same area may belong to different owners, so competitions between different EVCSs can be caused. This type of competition has been modeled by game-theoretic approaches in [1], [2], [4], and [5]. A supermodular game is proposed in [4] to study the competition among EVCSs with renewable power generators. A large fleet of EVs is studied in a mean-field game model to minimize their charging cost in [5]. Yang *et al.* [6] proposed an optimal EV route model based on a learnable partheno-genetic algorithm to minimize the total distribution costs of the EV route. A decentralized policy is studied in [7] to assign EVs to a network of charging stations with the goal of minimizing the queueing time. However, little work has been done to formulate both the traffic flow and the competition of EVCSs into an integrated problem.

This paper proposes an integrated charging navigation framework, which is made up of the power system, transportation system, navigation system, EVCSs, and EVs. Based on this framework, a hierarchical game approach is proposed to optimize the strategies of both EVCSs and EVs at two levels. At the upper level of the hierarchical game, a non-cooperative game is proposed to model the competition between EVCSs and manage them in a decentralized fashion. Evolutionary games are formulated at the lower level to evolve the EVs'

Manuscript received February 16, 2015; revised June 9, 2015; accepted July 14, 2015. Paper no. TSG-00179-2015.

The authors are with the Department of Electrical Engineering and Computer Science, University of Wisconsin–Milwaukee, Milwaukee, WI 53211 USA (e-mail: l.f.wang@ieee.org).

Color versions of one or more of the figures in this paper are available online at http://ieeexplore.ieee.org.

Digital Object Identifier 10.1109/TSG.2015.2458863

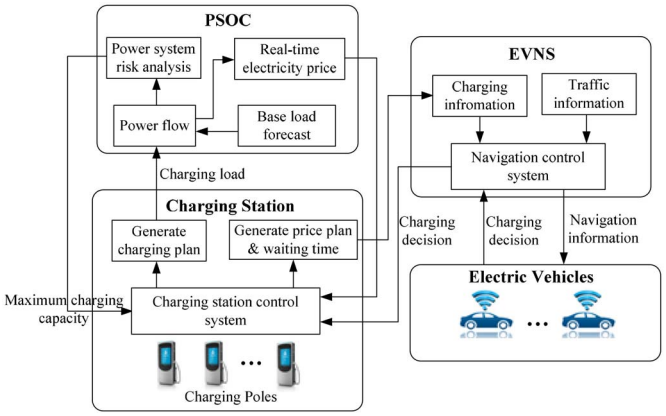

Fig. 1. Integrated EVs charging navigation framework.

strategies in choosing EVCSs. To solve the non-cooperative game, a particle swarm optimization (PSO) learning based best response algorithm is developed, which is able to improve the economic benefits and reduce the peak load of the power grid at the same time.

This paper has made contributions in the following aspects.

1) We proposed an integrated charging navigation framework to link the power system with transportation system. Thus, an optimal charging navigation strategy can be achieved to benefit both the power system and transportation system.
2) We developed a traffic flow simulation method for EVs considering the real-world usage data of EVs.
3) We proposed a novel business model for EVCSs based on game theory. Thus, the competition between charging stations can be modeled.
4) We developed an artificial intelligence learning based best response algorithm for the formulated game problem. Based on the intelligent algorithm, the approximated Nash equilibrium can be efficiently found.

The remainder of this paper is organized as follows. In Section II, the proposed integrated charging navigation system is introduced in detail. In Section III, we proposed a hierarchical game approach to coordinate the pricing strategies of charging stations and evolve the strategies of EVs in choosing EVCSs. Various simulations are carried out in Section IV to prove the effectiveness and benefits of the proposed hierarchical game approach. Finally, conclusions are drawn in Section V.

II. System Modeling

A. System Architecture

To study the impacts from both the power system and transportation system in the EV charging process, we proposed an integrated EV charging navigation framework as shown in Fig. 1. The integrated EV charging navigation framework comprises four major parts: 1) power system operation center (PSOC); 2) EVCSs; 3) electric vehicle navigation system (EVNS); and 4) EV terminals.

EVNS is responsible for collecting information and building connections between EVs and EVCSs. EVNS receives information from the EVCSs including the charging price and the estimated waiting time. It also collects current traffic information. Then the EVNS will broadcast the information to EVs. Upon receiving the information, EVs will decide if there is a need to charge and which EVCS should be selected (with the help of EVNS), as well as arrange the related charging activities. PSOC provides time of use (TOU) electricity prices to EVCSs based on the current load demand. Also it controls the maximum charging capacity of EVCSs to reduce the risk imposed on the power system.

B. Traffic Flow Model

The time horizon of the proposed control system is discretized into k time slots. During each time slot $t \in [k \cdot \Delta T,\ (k+1) \cdot \Delta T]$, $(k = 0, 1, 2, \ldots, K)$, the traffic flow is calculated to provide necessary traffic information to the EVNS. In a destination-oriented traffic system, the EVNS needs the information on the lengths of the routes and traffic speeds to navigate vehicles. Thus, we are focused on obtaining the traffic speeds of the lanes between neighboring traffic nodes. Three key variables in this traffic flow model are defined as follows: 1) traffic density $\rho_m(k)$ (veh/mile/lane), which is the number of vehicles in lane m during time slot k; 2) traffic speed $v_m(k)$ (mile/h), which is the average speed of the vehicles in lane m during time slot k; and 3) traffic flow $q_m(k)$ (veh/h), which is the number of vehicles leaving lane m during time slot k.

The traffic density of a lane is affected by the traffic flow as well as the start and end statuses of trips in this lane. The traffic density at time $(k+1)\Delta T$ is the sum of traffic density at time $k\Delta T$ and the increment of traffic density during time slot k. The traffic flows into the lane m can be expressed as $\sum_{\mu \in I_m} \beta_{\mu,m}(k) \cdot q_\mu(k)$ and the traffic flows out of the lane m is $\sum_{\varphi \in O_m} \beta_{m,\varphi}(k) \cdot q_\varphi(k)$, then the traffic density increment of lane m contribute by the traffic flow is $(\Delta T/L_m)(\sum_{\mu \in I_m} \beta_{\mu,m}(k) \cdot q_\mu(k) - \sum_{\varphi \in O_m} \beta_{m,\varphi}(k) \cdot q_\varphi(k))$. The traffic density increment of lane m due to the start and end statuses of trips can be expressed as $(1/L_m)(N_m^s(k) - N_m^E(k))$.

Thus, the traffic density can be expressed as follows:

$$\begin{aligned}\rho_m(k+1) = \rho_m(k) &+ \frac{\Delta T}{L_m}\left(\sum_{\mu \in I_m} \beta_{\mu,m}(k) \cdot q_\mu(k) - \sum_{\varphi \in O_m} \beta_{m,\varphi}(k) \cdot q_\varphi(k)\right) \\ &+ \frac{1}{L_m}\left(N_m^s(k) - N_m^E(k)\right) \end{aligned} \quad (1)$$

where I_m is the set of lanes entering lane m, $\beta_{\mu,m}$ is the turning rate of vehicles from lane μ into lane m, O_m is the set of lanes leaving lane m, L_m is the length of the lane m, $N_m^s(k)$ is the number of vehicles starting trips at lane m during time slot k, and $N_m^E(k)$ is the number of vehicles ending trips at lane m during time slot k.

The traffic speed can be calculated as follows [13]:

$$v_m(k) = v_m^f \cdot \exp\left[-\frac{1}{a_m}\left(\frac{\rho_m(k)}{\rho_{\mathrm{cr},m}}\right)^{a_m}\right] \quad (2)$$

where v_m^f is free-flow speed of lane m, $\rho_{\mathrm{cr},m}$ is the critical traffic density of lane m, and a_m is a statistical parameter. In the test system, we set $\rho_{\mathrm{cr},m} = 57.49$ (veh/mile/lane) and $a_m = 2.34$.

Based on the definition of traffic density $q_m(k)$, traffic flow $q_m(k)$, and traffic speed $v_m(k)$, the traffic flow can be naturally represented as follows:

$$q_m(k) = \rho_m(k) \cdot v_m(k). \tag{3}$$

To ensure that the traffic simulation is close to the real-world scenarios, we adopted the National Household Travel Survey (NHTS) 2009 [14] database to model the travel pattern of EVs. NHTS 2009 is the most comprehensive travel survey in U.S. available to date. It contains trip attributes such as trip start time, trip end time, and travel distance which can be used to generate the travel pattern. However, to simulate the traffic flow, spatial data should be added to the vehicle dataset. The spatial data contain the places where the vehicle starts and stops coupled with the travel route. The procedure for simulating the traffic flow can be elaborated as follows.

Step 1: Initialize all the vehicles in the simulated traffic system. The initial start places of vehicles are set randomly to be within the simulated area.

Step 2: Generate the start time, end time, and travel distance of each trip according to NHTS.

Step 3: Set the destination of each trip according to its travel distance and estimate the detailed driving route.

Step 4: Randomly select some vehicles as EVs from the simulated vehicles based on the EVs penetration level.

Step 5: Analyze the traffic flow of each lane in the transportation system using (1)–(3).

The detailed procedure for the traffic simulation of EVs is shown in Fig. 2. The EVs evaluate their current statuses at the beginning of each trip and make recharging decisions. If an EV finishes the charging process, it will continue the remaining trips of the day.

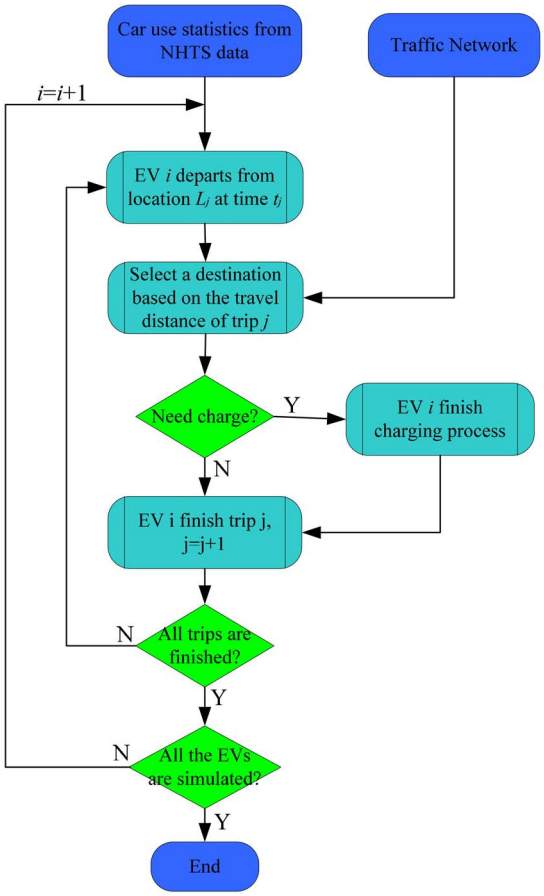

Fig. 2. Traffic simulation with real-time EV driving pattern.

C. Electric Vehicle Strategy

Multiple factors may affect the decisions of EVs, such as the SoC, charging price, the distance to the charging station, and the waiting time. When an EV receives the information from EVNS, it will make the decision on whether charge is needed or not. The charging probability is defined as follows:

$$p_j(k) = \begin{cases} 1, & \text{if } \mathrm{SoC}_{j,k} < 20\% \\ \exp\left[\dfrac{\mathrm{SoC}_{j,k} - 20\%}{\mathrm{SoC}_{j,k} - 100\%} \cdot \dfrac{a_p \cdot \sum_{i=1}^{I} r_{i,k}}{I \cdot r_{\max}}\right], & \text{if } 20\% \le \mathrm{SoC}_{j,k} < 100\% \end{cases} \tag{4}$$

where $\mathrm{SoC}_{j,k}$ is the SoC of EV j at time slot k, $r_{i,k}$ is the charging price of charging station i, $r_{\max}$ is the maximal limit of the charging price, I is the total number of charging stations, and a_p is vehicle charging probability parameters. We set $a_p = 0.8$ in this paper.

When the SoC of an EV is less than 20%, the charging probability will be 1 to avoid the depletion of battery during travel. Otherwise, the charging probability will be affected by the current SoC and the charging prices of EVCSs. As shown in (4), the charging probability of an EV will increase with the decrease in SoC and the decrease in average charging price. When SoC of an EV is close to 100%, the charging probability will be approximately 0%.

EVCSs can buy electricity at a relatively lower rate compared to the rate of home charging [4]. However, as the EVCS needs to make profit, the charging price may be higher for the EV owner compared to charging at home. Thus the EVs may not be fully charged through rapid charging at EVCSs, and we propose a model to optimally determine the energy needs to be purchased for an EV based on its current SoC and the charging price. We use quadratic utility function [15]–[17] to quantify the utility that an EV receives when charging at an EVCS as it is widely used in the literature. Without loss of generality, we design the quadratic utility function as follows:

$$u_{j,k}(E_{j,k}) = v_j \cdot E_{j,k} - \frac{\theta_j}{2} {E_{j,k}}^2, E_{j,k\min} \le E_{j,k} \le E_{j,k\max} \tag{5}$$

where v_j and θ_j are constant parameters for each EV, and $E_{j,k\min}$ and $E_{j,k\max}$ denote the minimal and maximal charging energy for the EV.

Clearly, the minimal and maximal charging energy of an EV is related with its current SoC and they are defined as follows:

$$E_{j,k\min} = \mathrm{Max}\left\{\mathrm{SoC}_{j,\min} \cdot \mathrm{Cap}_j + E_{\mathrm{res},j} - \mathrm{SoC}_{j,k} \cdot \mathrm{Cap}_j, 0\right\} \tag{6}$$

$$E_{j,k\max} = \left(1 - \mathrm{SoC}_{j,k}\right) \cdot \mathrm{Cap}_j \tag{7}$$

where $\mathrm{SoC}_{j,\min}$ is the minimal limit of the SoC of EV j, Cap_j is the battery capacity of EV j, $E_{\mathrm{res},j}$ is the estimated energy needed for the rest trips of EV j during the day, and $\mathrm{SoC}_{j,k}$ is the current SoC of EV j.

As EVs need to pay for the energy purchased at the EVCSs, the welfare function of an EV when charging at an EVCS can be described as follows:

$$w_{j,k}\left(E_{j,k}\right) = u_{j,k}\left(E_{j,k}\right) - r_{i,k}^{j} \cdot E_{j,k} \tag{8}$$

where $r_{i,k}^{j}$ is the charging price.

Thus, the optimal energy purchased of an EV j charging at EVCS i can be obtained as follows:

$$\begin{aligned} E_{j,k}^{*} &= \mathrm{argmax}_{E_{j,k}} w_{j,k}\left(E_{j,k}\right) \\ &= \begin{cases} E_{j,k\min}, & \text{if } \dfrac{v_j - r_{i,k}^{j}}{\theta_j} < E_{j,k\min} \\ \dfrac{v_j - r_{i,k}^{j}}{\theta_j}, & \text{if } E_{j,k\min} \le \dfrac{v_j - r_{i,k}^{j}}{\theta_j} \le E_{j,k\max} \\ E_{j,k\max}, & \text{if } E_{j,k\max} < \dfrac{v_j - r_{i,k}^{j}}{\theta_j}. \end{cases} \end{aligned} \tag{9}$$

Once an EV responds to the charging navigation signal, it has to choose a charging station and the charging station will hold the current charging price for the EV. An EV selects an EVCS based on its economic and time costs. The economic cost comprises the charging cost and the fuel cost. The time cost consists of the travel time and the waiting time. The travel time is the time used by the EV for traveling to the charging station which is certainly affected by the traffic flow. Thus, the cost of EV j selecting EVCS i can be expressed as follows:

$$\mathrm{cost}_{i,j} = \lambda t_{i,j}^{\mathrm{total}} + \left(E_{j,k}^{*} + d_{i,j} \cdot E_{\mathrm{travel}}\right) r_{i,k}^{j} \tag{10}$$

$$t_{i,j}^{\mathrm{total}} = t_{i,j}^{\mathrm{travel}} + E\left[W_Q\right] \tag{11}$$

where $t_{i,j}^{\mathrm{travel}}$ is the travel time of EV j to charging station i, $E[W_Q]$ is the estimated waiting time of EV j at charging station i, $r_{i,j}$ is the charging price, $d_{i,j}$ is the travel distance from the EV to the charging station, E_{travel} is the energy consumption per miles for EV, and λ is the weighting factor of the time cost.

D. Charging Station Strategy

We assume that the charging stations belong to different owners, and their only goal is to maximize their own profits.

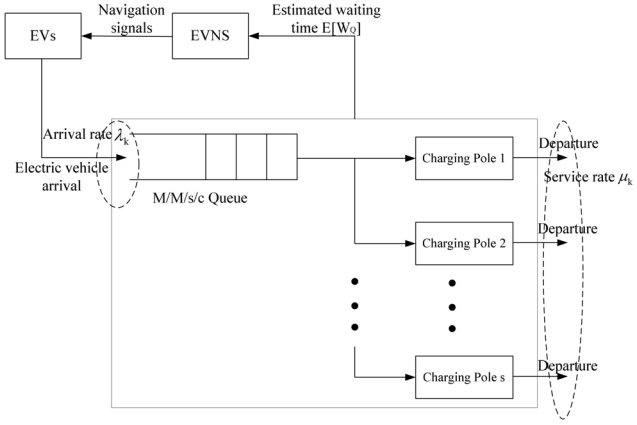

Fig. 3. EVs' queueing model at a charging station.

The EVCSs will compete with each other for attracting EVs to charge at their charging poles. Each EVCS has a limited number of charging poles s_i, $i \in I$. And if the number of EVs at an EVCS is more than the available charging poles, the EVs will wait in the queue. The number of available charging poles is dependent on the current state of the power distribution system. The charging capacity of the EVCSs is limited by the PSOC at the peak load time in order to reduce the risk of the power system as shown in Fig. 1. The EVCSs buy power from the power grid at a lower price and sell power to EVs at a higher price in order to make profits.

In order to reduce the peak load of the system, a vTOU rate policy is developed based on the system load demand for encouraging EVCSs to attract EVs to charge at off-peak times. The electricity price is defined as follows:

$$\rho_k = \alpha \cdot P_{\mathrm{sys}}^{t} \tag{12}$$

where α is price parameters and P_{sys}^{t} is the load demand of the system at time slot t.

According to (12), the electricity price is higher at the peak-load hours. Thus, the EVCSs will offer higher charging prices and there is a lower probability for EVs to charge during these time periods. As a result, the charge load can be shifted to off-peak hours based on this pricing policy.

EVCSs' strategies are the charging prices at each time slot which are denoted as follows:

$$\pi_i = \left[r_{i,0}, r_{i,1}, \ldots, r_{i,k}, \ldots, r_{i,K}\right], \ \forall i \in I. \tag{13}$$

The revenue of an EVCS can be expressed as follows:

$$U_i = \sum_{k=1}^{K} \left(\sum_{j=1}^{N_{i,k}} E_{j,k}^{\mathrm{i}*} \cdot r_{i,k} - P_k^i \ \cdot \rho_k \right) \tag{14}$$

where $N_{i,k}$ is the total number of EVs choosing EVCS i at time slot k, and P_k^i is the total charging load of EVCS i at time slot k.

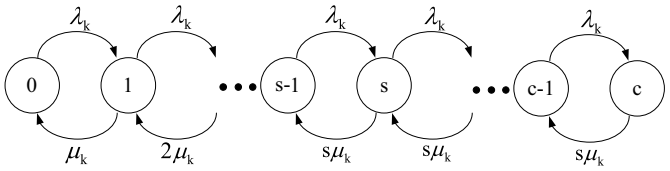

Fig. 4. State transition diagram of the queueing model.

E. EVs' Queueing Model

In the proposed integrated EV navigation system, EVs will wait in a queue if all the charging poles are occupied at an EVCS and the EVCS will announce its estimated waiting time to EVs which need to make charging decisions.

In this section, we model the queueing process of EVs at a charging station as an M/M/s/c queue [18], [19]. The queueing model is shown in Fig. 3. The proposed M/M/s/c queue is a multiserver queue with s identical servers and a maximum queueing length of c. In the queueing model, each charging pole can be viewed as a server and the customers are the EVs. As shown in the figure, the EVs are served based on a first-come-first-serve rule. The waiting time is estimated based on the queueing model and it is broadcasted to EVs through EVNS to help the EVs make charging decisions.

In this paper, EVs' strategies in choosing EVCSs are affected by the pricing strategies of the charging stations. We will formulate an evolutionary game to evolve the EVs strategies in choosing EVCSs in the next section and the arrival rate of EVs at a certain EVCS λ_k is derived accordingly. As service rate of the charging poles is not affected by the strategies of EVCSs, it is assumed to follow an exponential distribution. At each time slot, the queue will evolve to a stable state and the waiting time can be estimated.

The evolving process of the proposed queueing model is based on a birth-death process and its state transition diagram is shown in Fig. 4. As shown in the figure, the states indicate the number of EVs in the queue. If the number of EVs in the charging station n is less than the number of charging poles s, then the departure rate of EVs is $n\mu_k$; if $s < n \le c$, the departure rate is $s\mu_k$ as there are only s servers in the queueing system.

The transition matrix of the queueing system $\boldsymbol{P}$ is shown in (15), shown at the bottom of this page. Let $\overline{\Pi} = [\Pi_1, \Pi_2, \dots \Pi_s, \dots]$ denote the stationary distribution vector. Then, the stationary condition of the queueing system can be expressed as follows:

$$\overline{\Pi} \cdot P_k = 0. \tag{16}$$

Let $A = \lambda_k/\mu_k$. We can obtain the following steady-state equations based on (16).

For state 1: $\Pi_1 = A\Pi_0$.
For state 2: $\Pi_2 = A\Pi_1/2 = A^2\Pi_0/2!$.
For state 3: $\Pi_3 = A\Pi_2/3 = A^3\Pi_0/3!$.
For state s: $\Pi_s = A\Pi_{s-1}/s = A^s\Pi_0/s!$.
For state $s+1$: $\Pi_{s+1} = A\Pi_s/s = A^{s+1}\Pi_0/(s!\,s)$.
For state $s+2$: $\Pi_{s+2} = A\Pi_{s+1}/s = A^{s+2}\Pi_0/(s!\,s^2)$.
For state c: $\Pi_c = A\Pi_{c-1}/s = A^c\Pi_0/(s!\,s^{c-s})$.
Then we can conclude the stationary distribution as follows:

$$\Pi_n = \begin{cases} \dfrac{A^n\Pi_0}{n!}, & \text{if } 0 \le n \le s \\ \dfrac{A^s}{s!}\left(\dfrac{A}{s}\right)^{n-s}\Pi_0, & \text{if } s < n \le c. \end{cases} \tag{17}$$

Consider the constraint of the stationary distribution

$$\sum_{n=0}^{c} \Pi_n = 1. \tag{18}$$

We can obtain

$$\Pi_0 = \left(\sum_{n=0}^{s-1}\frac{A^n}{n!} + \frac{A^s}{s!}\sum_{n=s}^{c}\left(\frac{A}{s}\right)^{n-s}\right)^{-1}. \tag{19}$$

The mean queue length is derived as follows [18]:

$$E[N_Q] = \sum_{n=s+1}^{c}(n-s)\Pi_n. \tag{20}$$

The waiting time can be derived by Little's formula [18] as follows:

$$E[W_Q] = \frac{E[N_Q]}{\lambda_k(1-\Pi_c)}. \tag{21}$$

F. EVs' Impact on Distribution System Reliability

EVs can affect the reliability of a distribution system by overloading the transformers and transmission lines at peak load hours. Thus, a real-time transformer outage rate is needed to evaluate the impact of EVs on distribution system reliability. Instead of using a constant outage rate, we formulate the operational reliability of the distribution network by considering

$$P_k = \begin{bmatrix} -\lambda_k & \lambda_k & 0 & 0 & 0 & 0 & \cdot & \dots & \cdot \\ \mu_k & -(\mu_k+\lambda_k) & \lambda_k & 0 & 0 & 0 & \cdot & \dots & \cdot \\ 0 & 2\mu_k & -(2\mu_k+\lambda_k) & \lambda_k & 0 & 0 & \cdot & \cdots & \cdot \\ 0 & 0 & 3\mu_k & -(3\mu_k+\lambda_k) & \lambda_k & 0 & \cdot & \dots & \cdot \\ \cdot & \dots & \cdot & \ddots & \ddots & \ddots & \cdot & \dots & \cdot \\ \cdot & \dots & \cdot & \dots & s\mu_k & -(s\mu_k+\lambda_k) & \lambda_k & \dots & \cdot \\ \cdot & \dots & \cdot & \dots & \cdot & s\mu_k & -(s\mu_k+\lambda_k) & \lambda_k & \dots \\ \cdot & \dots & \cdot & \dots & \cdot & \dots & \ddots & \cdot & \dots \\ \cdot & \dots & \cdot & \dots & \cdot & \dots & s\mu_k & -(s\mu_k+\lambda_k) & \lambda_k \end{bmatrix} \tag{15}$$

the real-time outage rate of the distribution transformer. The hybrid transformer failure probability model can be expressed as follows based on [20]:

$$P_f = 1 - (1 - P_{\text{rand}}) \times (1 - P_{\text{af}}) \tag{22}$$

where P_{rand} is the random failure probability and P_{af} is the transformer aging failure under various load conditions.

The current-dependent overload protection outage rate can be obtained through (23)–(25) [20]

$$P_{\text{pt}}(I) = \begin{cases} P_{\text{unreq}}, & \text{if } I < I_{\text{pe}}(1-\varepsilon_I) \\ P_{\text{req}} \int_{I_{\text{pe}}(1-\varepsilon_I)}^{I} f(I_{\text{pk}}) dI_{\text{pk}} + P_{\text{unreq}} \int_{I}^{I_{\text{pe}}(1+\varepsilon_I)} & \\ \quad f(I_{\text{pk}}) dI_{\text{pk}}, & \text{if } I_{\text{pe}}(1-\varepsilon_I) < I < I_{\text{pe}}(1+\varepsilon_I) \\ P_{\text{req}}, & \text{if } I > I_{\text{pe}}(1+\varepsilon_I) \end{cases} \tag{23}$$

$$f(I_{\text{pk}}) = \begin{cases} 0, & \text{if } I_{\text{pk}} < I_{\text{pe}}(1-\varepsilon_I) \\ & \quad \text{or } I_{\text{pk}} > I_{\text{pe}}(1+\varepsilon_I) \\ \dfrac{e^{\left(-(I_{\text{pk}}-I_{\text{pe}})^2 / 2\sigma^2\right)}}{\alpha_I \sigma \sqrt{2\pi}}, & \text{if } I_{\text{pe}}(1-\varepsilon_I) < I_{\text{pk}} < I_{\text{pe}}(1+\varepsilon_I) \end{cases} \tag{24}$$

$$\alpha_I = \phi\left(\frac{\varepsilon_I I_{\text{pe}}}{\sigma}\right) - \phi\left(\frac{-\varepsilon_I I_{\text{pe}}}{\sigma}\right) \tag{25}$$

where ϕ is the cumulative distribution function of the standard normal distribution, P_{unreq} is the outage rate when the overload protection is not required, P_{req} is the outage rate when the overload protection is required, I_{pk} is pick-up current for the protection relay, I_{pe} is the expected value of I_{pk}, σ is standard variance of I_{pk}, and ε_I is the percentage error of current mismatch.

Thus, the real-time transformer outage rate can be built by considering both the failure rate and overload protection rate as follows:

$$P^t_{\text{trans}} = 1 - \big(1 - P_f(t)\big) \times \big(1 - P_{\text{pt}}(I_t)\big). \tag{26}$$

III. Hierarchical Game Formulation

The proposed hierarchical game framework consists of two levels of games. At the upper level, a non-cooperative game is formulated to coordinate the pricing strategies of EVCSs to maximize their personal profits. Based on the pricing strategies of EVCSs, multiple evolutionary games are formulated at the lower level for different groups of EVs to evolve their strategies in choosing EVCSs. During each step of the noncooperative game, an evolutionary equilibrium will be reached for each evolutionary game at the lower level and the EVs' strategies in choosing EVCSs are optimized. Once the Nash equilibrium is reached for the non-cooperative game, the games at the two levels will both reach their equilibriums. Then the strategies for both EVs and EVCSs are optimized and the solution to the formulated problem is found.

A. Evolutionary Games of EVs

Currently, EVs are considered as price takers by researchers in the charging navigation problem as the charging decision of one EV does not have enough power to affect pricing strategies of the charging stations [4]–[7]. However, with the development of the connected vehicle technology, EVs may be able to cooperate with each other and bid charging prices as a group. Thus, EVs can work together as a group to negotiate charging prices with charging stations. In the proposed integrated charging navigation framework, EVs can cooperate with their neighboring EVs to bargain charging prices with EVCSs as a group. We assign the EVs at the same lane into one group as they have similar travel distance to different EVCSs. The strategy evolving of each EV group is guided by an evolutionary game.

Two important concepts in evolutionary games are replicator dynamics and population [21]. In the context of evolutionary games, the population refers to a set of players with the same strategy and the population share is the percentage of the population with a certain strategy. The replicator dynamics controls the reproduction speed of the population according to the payoff of the population's strategy. In the proposed evolutionary game, each EV has to choose a charging station to recharge its battery and it can gradually evolve its strategy based on the current pricing strategies of EVCSs. Thus, the population share is defined as the probability distribution of an EV choosing different EVCSs. Based on evolution strategy (ES), we propose a replicator dynamics to guide the evolution of the population share.

Based on the traffic simulation model, we can obtain the number EVs at time slot k in lane m which is denoted as $N^T_{m,k}$. Then the number of players in the m_{th} evolutionary game is

$$N_{m,k} = N^T_{m,k} \cdot p_j(k) \tag{27}$$

where $p_j(k)$ is the charging probability of EVs at time slot k.

Let $y^i_{m,k}$ denote the probability of an EV choosing to charge at EVCS i at time slot k, where $0 \le y^i_{m,k} \le 1$ and $\sum_{i=1}^{I} y^i_{m,k} = 1$. Thus, we can denote the population share as $Y_k = [y^1_{m,k}, y^2_{m,k}, \ldots, y^i_{m,k}, \ldots, y^I_{m,k}]$. Then we can define the accumulated EVs' utility choosing EVCS i as follows:

$$U^{\text{EV}}_{i,m} = -\sum_{j=1}^{N_{m,k}} \left[\lambda t^{\text{total}}_{i,j} + \left(E^*_{j,k} + d_{i,j} \cdot E_{\text{travel}}\right) r^j_{i,k}\right] \tag{28}$$

where $t^{\text{total}}_{i,j} = t^{\text{travel}}_{i,j} + E[W_{Q,i}]$.

The average utility of choosing different EVCSs is denoted as follows:

$$\overline{U}^{\text{EV}}_m = \sum_{i=1}^{I} y^i_{m,k} U^{\text{EV}}_{i,m}. \tag{29}$$

Accordingly, the replicator dynamics can be defined as follows:

$$\frac{\partial y^i_{m,k}}{\partial t} = \delta y^i_{m,k}\left(U^{\text{EV}}_{i,m} - \overline{U}^{\text{EV}}_m\right), \ \forall i \in I \tag{30}$$

where δ is the learning rate of the replicator dynamics.

Note that the probability of an EV choosing EVCS i will increase when the utility for choosing EVCS i is larger than the average utility, and vice versa. Thus, the proposed replicator dynamics can maximize the utility of the EVs.

The evolutionary equilibrium is the solution of evolutionary game which is a stable condition that the strategy state

stops evolving. For the formulated problem, the evolutionary equilibrium is reached when

$$\frac{\partial y^i_{m,k}}{\partial t} = \dot{y}^i_{m,k} = 0, \ \forall i \in I \tag{31}$$

$$\Pi^{\mathrm{EV}}_i = \overline{\Pi}^{\mathrm{EV}}, \ \forall i \in I. \tag{32}$$

The evolutionary equilibrium is denoted by $Y^*_{m,k} = [y^{1*}_{m,k}, y^{2*}_{m,k}, \ldots, y^{i*}_{m,k}, \ldots, y^{I*}_{m,k}]$.

When the evolutionary equilibriums of all the evolutionary games are reached, the optimal strategies of all the EVs are obtained and arrival rate of EVs can be calculated.

The arrival rate of EVs at EVCS i can be expressed as follows:

$$\lambda_{i,k} = \sum_{m=1}^{M} N_{m,k} \cdot y^{i*}_{m,k} \tag{33}$$

B. Non-Cooperative Game of EVCSs

1) Non-cooperative Game Formulation: In this section, we formulate a price adjustment game for multiple EVCSs. To coordinate the set of $I (I = [1, 2, \ldots, I])$ EVCSs, a non-cooperative EVCS interaction game $\mathbb{G}$ is defined as follows.

1) *Players:* The set of all I EVCSs.
2) *Strategies:* For each EVCS, choose a charging price strategy $\pi_i, \forall \pi_i \in \boldsymbol{F}_i$.
3) *Payoffs:* The i_{th} EVCS receives payment $U_i(\pi_i, \pi_{-i})$ as shown in (14).

The most common solution for a non-cooperative game is the Nash equilibrium which is defined as follows.

Definition 1: For the proposed non-cooperative game $\mathbb{G} = \{I, \{\pi_i\}_{i\in I}, \{U_i\}_{i\in I}\}$, a strategy tuple $\Psi = \{\pi^*_i\}_{i\in I}$ constitutes a Nash equilibrium when no player can improve its utility by unilaterally deviating from its current strategy. It is formulated as a set of inequalities

$$U_i\left(\pi^*_i, \pi^*_{-i}\right) \geq U_i\left(\pi_i, \pi^*_{-i}\right), \ \forall \pi_i \in \boldsymbol{F}_i, \ \forall i \in I. \tag{34}$$

The existence of a unique Nash equilibrium is uncertain in a general non-cooperative game [22]. We hereby included a small positive variable ε_1 to get an approximate Nash equilibrium as described in (35) [23]. As the approximate Nash equilibrium results in a similar performance and it can reduce the computational time of the best response strategy [23], it can be used as the solution of the proposed non-cooperative game

$$U_i\left(\pi^*_i, \pi^*_{-i}\right) \geq U_i\left(\pi_i, \pi^*_{-i}\right) - \varepsilon_1, \ \forall \pi_i \in \boldsymbol{F}_i, \ \forall i \in I. \tag{35}$$

2) Proposed Algorithm: To find the Nash equilibrium for the proposed game $\mathbb{G}$, we applied a dynamic best response strategy which is defined as follows.

Definition 2: For each player $i \in \boldsymbol{\mathcal{M}}$, while other players have a fixed strategy tuple π_{-i}, the best response strategy π'_i for the ith player is

$$\pi'_i = \mathrm{argmax}_{\pi_i \in \boldsymbol{F}_i}\{U_i(\pi_i, \ \pi_{-i})\}. \tag{36}$$

Thus, the players will continue to update their strategies based on the strategies of other players in a sequential and iterative fashion. This dynamic response process continues until the approximated Nash equilibrium is reached.

As the payoff function of the proposed game is nonlinear, analytical methods such as dynamic programing is not applicable. The strategies described in (13) constitute a very large search space, so enumeration method is also not applicable. Thus, computational intelligence methods have been used by researchers to search the Nash equilibrium [24]. To solve the formulated game, we applied two artificial intelligence based algorithms, namely PSO [25] and ES, to find the best response strategy for each player. The performances of these two algorithms are studied and compared in the simulation studies.

The reason of using PSO is because it is very suitable for this problem. In this problem, the control variable is the charging prices of the EVCSs. The charging price vector of an EVCS can be mapped into a search space and the charging prices at each time slot can be naturally viewed as different dimensions in the search space. The value of the charging price can be encoded as the coordinates in the specified dimension. Another suitable algorithm for this problem is ES, as the data structure of ES corresponds to real-valued vectors.

a) PSO algorithm: PSO originates from the collective behaviors exhibited in bird flocking and fish schooling. In PSO, the possible solution of a target problem is mapped into a search space and the locations of the particle in the search are the potential solutions to the problem. The particles continuously update their locations and velocities in the search space according to (37)–(39). The fitness of each potential solution is evaluated by an objective function. If an optimum value is reached for a specific particle, the position of the particle will be stored as a personal best position pBest. And if an optimum value is reached for all the particles, the position of this particle will be saved as a global best position gBest. When the iteration is over, the best value position gBest can be found to optimize the objective function

$$v^{m+1}_{id} = w v^m_{id} + C_1 \cdot \mathrm{rand}_1 \cdot \left(\mathrm{pBest}_i - x^m_{id}\right) + C_2 \cdot \mathrm{rand}_2 \cdot \left(\mathrm{gBest} - x^m_{id}\right) \tag{37}$$

$$x^{m+1}_{id} = x^m_{id} + v^{m+1}_{id} \tag{38}$$

$$w = w_{\max} - m \cdot \frac{w_{\max} - w_{\min}}{k_{\max}} \tag{39}$$

where v_{id} is the velocity of particle i at dimension d, x_{id} is the position of particle i along dimension d, w is the inertia weight, and m is the iteration number.

In this specific problem, we need to find the best response strategy of the ith charging station $\pi'_i = [r_{i,0}, r_{i,1}, \ldots, r_{i,k}, \ldots, r_{i,K}]$. The charging price at each time slot can be defined as a dimension of the search space, and the range of the specific charging price can be encoded as the coordinates in the specified dimension. The objective function is to maximize the payoff of the charging station as shown in (14). Solving the problem is equivalent to finding the optimal location in the search space.

The computational procedure of the PSO algorithm can be elaborated as follows.

Step 1: Initialize all the particles in the search space. Particle positions and velocities are set randomly to be within the feasible search space.

Algorithm 1 Best Response Algorithm for the Non-cooperative Game

1: **Input** randomly initialize strategies for all players.
2: **repeat**
3: **for** $i = 1, \ldots, I$ **do**
4: The player i finds its current best response strategy π_i' based on (36). Then the player provides other players with its current best response strategy π_i'.
5: **end for**
6: **until** the approximate Nash equilibrium (35) is reached.
7: Output control strategies and stop.

Step 2: Evaluate the fitness of each original particle with respect to the objective function (14).
Step 3: Compute the fitness value of each particle; and if it is a better solution for this particle, then store its position as a pBest position for this specific particle.
Step 4: Check the fitness value of each particle. If it is the best solution for all particles, then store the particle's position as gBest position.
Step 5: Update the position and velocity of each particle according to (37)-(39).
Step 6: If $v_{ik}^m > V_{\max}$, then $v_{ik}^m = V_{\max}$; If $v_{ik}^m < V_{\min}$, then $v_{ik}^m = V_{\min}$; If $x_{ik}^m > X_{\max}$, then $x_{ik}^m = X_{\max}$; If $x_{ik}^m < X_{\min}$, then $x_{ik}^m = X_{\min}$.
Step 7: If the stopping criterion is satisfied, then go to step 8; otherwise, go to step 2.
Step 8: Output the optimal solution.

b) Evolution strategy: The ES used in this paper is operated with a single individual in the population subjected to mutation.

In this problem, the charging price vector of an EVCS $\pi_i' = [r_{i,0}, r_{i,1}, \ldots, r_{i,k}, \ldots, r_{i,K}]$ is encoded into a chromosome as $\mathbf{x} = [x_0, x_1, \ldots, x_k, \ldots, x_K, \sigma]$. The standard deviations of all attributes of $\mathbf{x}$ are identical, and they are mutated as follows:

$$\sigma^{t+1} = \sigma^t \exp \in (\tau_0 \cdot N(0,1)) \quad (40)$$

$$x_k^{t+1} = x_k^t + \sigma^{t+1} \cdot N(0,1) \quad (41)$$

where τ_0 is the learning rate and $\tau_0 \propto K^{-1/2}$.

The fitness of the chromosome is evaluated by the payoff of the EVCS as shown in (14). If the mutated chromosome has a higher fitness value, then replace the current chromosome with the mutated chromosome. Otherwise, keep the chromosome unchanged. This process goes until the stopping criterion is satisfied. The chromosome obtained in the ES is the optimal strategy for the EVCS.

The proposed best response algorithm is summarized in Algorithm 1 as follows.

In Algorithm 1, each player is required to provide its current best response strategy to other players. Thus, it is possible that the player may cheat other players by injecting untruthful information if cheating can increase its utility. However, we will show that all the players will provide truthful information about their best response strategies in Theorem 1.

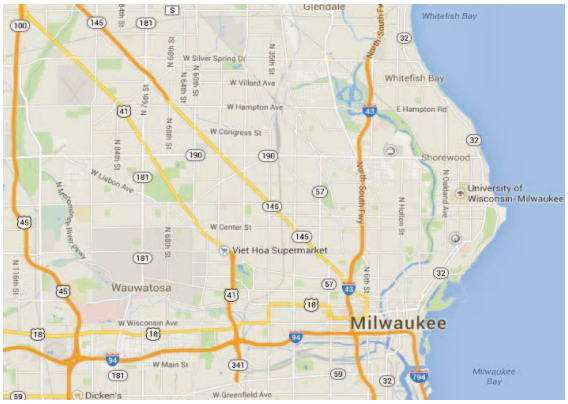

Transportation Network

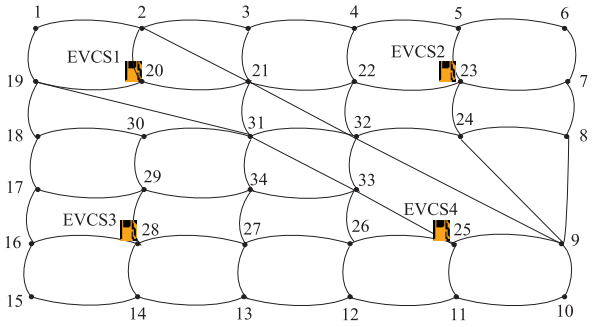

Topological Graph

Fig. 5. Topology of the transportation network under test.

Theorem 1: In Algorithm 1, no player can benefit by misreporting its best response strategy. That is, the players are self-enforced to provide their truthful strategy information.

Proof: To prove the theorem, it suffices to show that a player's best choice is to provide its true strategy information when other players reveal their true strategy information.

Let $\pi_1^*, \ldots, \pi_i^*, \ldots, \pi_I^*$ denote the Nash equilibrium of the non-cooperative game when all the players provide truthful information. Denote $\pi_1^*, \ldots, \overline{\pi}_i, \ldots, \pi_I^*$ as the Nash equilibrium reached when player i provides untruthful information about its strategy $\overline{\pi}_i$. We denote the utility of player i when providing truthful and untruthful information as U_i^* and $\overline{U}_i$, respectively.

Based on the definition of best response strategy we have $\pi_i^* = \pi_i' = \text{argmax}_{\pi_i \in \boldsymbol{F}_i}\{U_i(\pi_i, \pi_{-i}^*)\}$ which means $\forall \pi_i \in \boldsymbol{F}_i$, $\forall i \in I$, $U_i^* \geq \overline{U}_i$. That is, the player i cannot benefit by misreporting its best response strategy. Therefore, we can conclude that all the players in Algorithm 1 will provide their truthful best response strategy. ■

IV. Case Studies

A. Simulation Environment

Simulation studies are performed based on the transportation network of Milwaukee, Wisconsin. Fig. 5 shows the transportation network and its topological graph. Four EVCSs are located at traffic nodes 20, 23, 25, and 28. The free-flow traffic speed is 30 miles/h. The traffic flow simulation considers 50 000 vehicles and 5% of them are EVs. The topology of

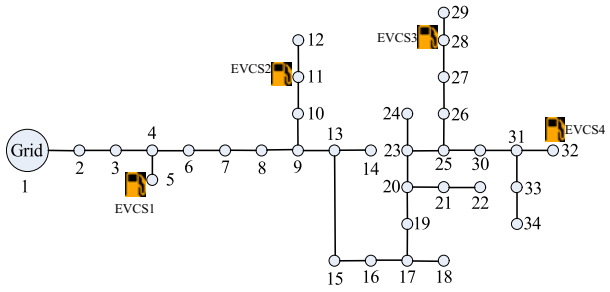

Fig. 6. Topology of the studied residential distribution grid.

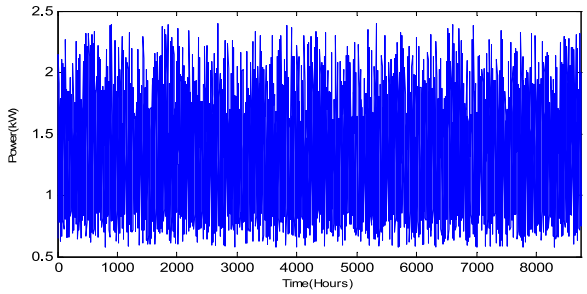

Fig. 7. Annual load profile for a single household.

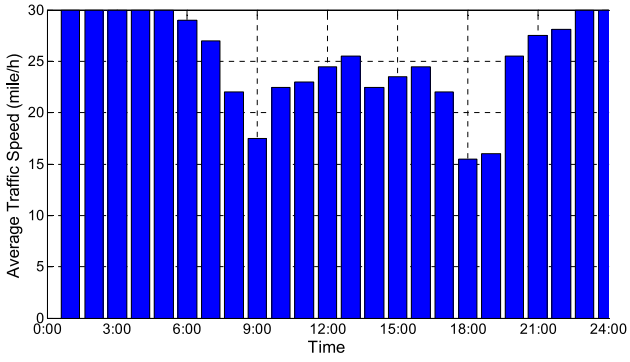

Fig. 8. Average traffic speed of the test system.

the studied distribution system is based on the IEEE 34-node test feeder [26] as shown in Fig. 6. Four EVCSs are connected to four load points which are labeled from EVCS1 to EVCS4 in the figure. Assume a transformer is located at Node 1 and 2500 houses are randomly located at other nodes. The load profile of a single household is shown in Fig. 7 and the base load in the distribution system consists of the load of 2500 households. Assume the interruption rates for the main feeder and lateral feeder are 0.1 interruptions/year and 0.2 interruptions/year, respectively; the average times to repair for the main feeder and lateral feeder are 2.5 h and 1 h, respectively. The procedure for reliability analysis is based on Monte Carlo simulation and can be found in our previous work [27]. The shortest route navigation approach is used as a benchmarking control strategy. In this strategy, EVs are guided to the nearest EVCS for recharging their batteries when their SoCs are below 40%.

B. Simulation Results

Fig. 8 shows the simulation results of the average traffic speed of the transportation system during a day.

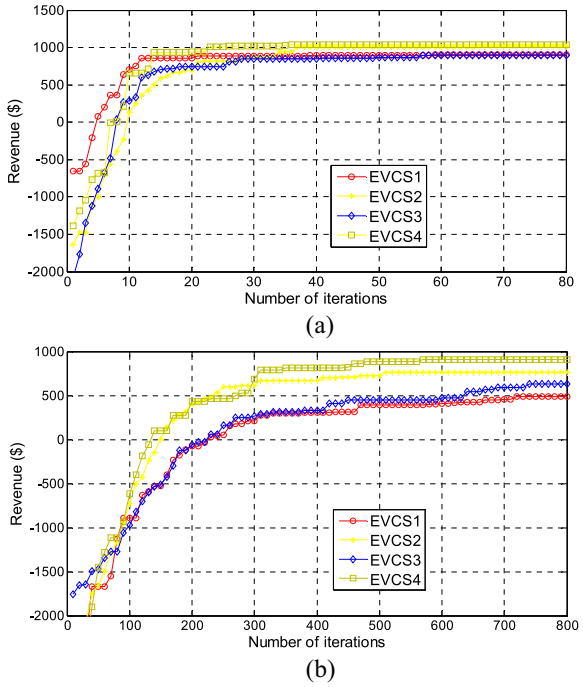

Fig. 9. Convergence curves of different response algorithms in a best response iteration. (a) PSO algorithm. (b) ES.

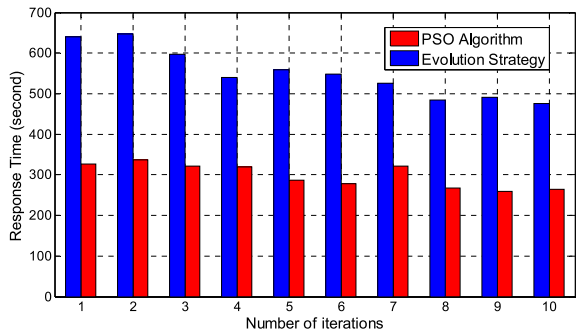

Fig. 10. Response time of different response algorithms during the iterations of the non-cooperative game.

The traffic conditions vary during the day time. The traffic is most congested during 8:00–10:00 and 17:00–19:00 when most people commute to/from the working places. Fig. 9 shows the convergence curves of the PSO algorithm and ES during an iteration of the best response algorithm. The response algorithms search the best response strategy for the player after other players choose their strategies. It ensures the effectiveness of the proposed best response algorithm in finding the Nash equilibrium. As shown in Fig. 9, PSO algorithm converges faster and results in higher revenues compared with the ES. The response time of PSO algorithm is also shorter than ES as shown in Fig. 10. Thus, the PSO algorithm is used for searching the best response strategies in the proposed non-cooperative game. The convergence behavior of the proposed non-cooperative game approach is shown in Fig. 11. As shown in the figure, the payoffs of all the players converge to a stable state after several iterations. Thus, the approximate Nash equilibrium has been reached, and the EVCSs will not deviate from their current price strategies. Their revenues reach a stable state after competing with each other.

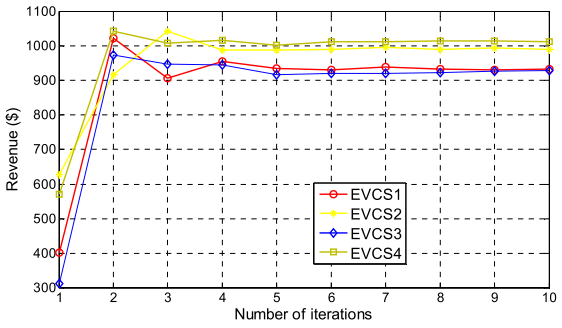

Fig. 11. Convergence of the non-cooperative game.

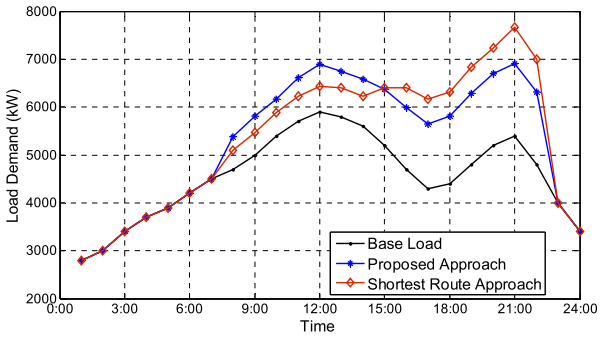

Fig. 12. Load demand curves of the system with different EV navigation strategies.

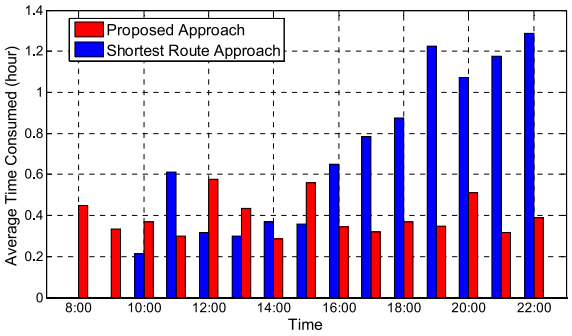

Fig. 13. Average time consumed by EVs with different navigation strategies at different time windows.

Fig. 12 shows the load demand of the system. The charging load incurred by EVCSs increases the peak load of the system. Compared with the shortest route navigation approach, the proposed integrated navigation approach reduced the burden of the peak load by attracting more EVs to charge at off-peak hours when the electricity price is lower. Fig. 13 gives the average time consumed by EVs to recharge their batteries. The time consumed by EVs comprises the travel time to EVCSs and the waiting time at the EVCSs. As shown in the figure, the proposed integrated navigation approach results in less average time consumed. As the proposed approach provides the EVs with the information on the traffic conditions and the estimated waiting time at different EVCSs, the EVs will not only save travel time by avoiding congested routes but also reduce waiting time by selecting a less crowded EVCS. The reliability indices of the residential distribution system under different navigation approaches are shown in Table I. The reliability metrics used in Table I are system average interruption frequency index (SAIFI), system average interruption duration index (SAIDI), customer average interruption duration index (CAIDI), and average service availability index (ASAI) [28]. SAIFI is the average instances of interruption per customer experienced per year due to the failure of the system components. SAIDI is the average outage duration per customer suffered per year. The unit of SAIDI is hour/system customer/year. CAIDI is the average outage duration of those customer interruptions, and its unit is hour/customer interruption. ASAI is the ratio of customer hours of available service and the customer hours demanded per year and the unit is 100%. Base on the results in Table I, it can be concluded that the proposed approach has a positive impact on the reliability indices. The values of SAIFI, SAIDI, and CAIDI are considerably decreased compared with the shortest route approach.

TABLE I
RELIABILITY INDICES FOR THE RESIDENTIAL DISTRIBUTION SYSTEM UNDER DIFFERENT NAVIGATION APPROACHES

	SAIFI	SAIDI	CAIDI	ASAI
Shortest Route Approach	51.23	808.64	15.78	0.9077
Proposed Approach	1.079	5.364	4.971	0.9994

V. CONCLUSION

This paper proposes an integrated framework for real-time EV navigation, which considers both the impacts from the transportation system and power system. Under the proposed framework, the competition between EVCSs is modeled with a non-cooperative game approach. A novel algorithm is also developed to solve the formulated game. Finally, the simulation results demonstrate that the proposed approach is effective in improving both the economic benefits of the charging stations and the reliability of the power grid.

This paper can be further extended in multiple directions. One research direction is to find the optimal locations of charging stations. The placement of charging stations in a city area may have impacts on both the traffic flow and power system reliability. Future study may consider both the optimal location and optimal control strategies of charging stations to make it an integrated problem.

REFERENCES

[1] W. Lee, L. Xiang, R. Schober, and V. W. S. Wong, "Analysis of the behavior of electric vehicle charging stations with renewable generations," in *Proc. IEEE Conf. Smart Grid Commun.*, Vancouver, BC, Canada, 2013, pp. 145–150.

[2] J. Escudero-Garzas and G. Seco-Granados, "Charging station selection optimization for plug-in electric vehicles: An oligopolistic game-theoretic framework," in *Proc. IEEE Conf. PES Innov. Smart Grid Technol. (ISGT)*, Washington, DC, USA, 2012, pp. 1–8.

[3] Q. Guo, S. Xin, H. Sun, Z. Li, and B. Zhang, "Rapid-charging navigation of electric vehicles based on real-time power systems and traffic data," *IEEE Trans. Smart Grid*, vol. 5, no. 4, pp. 1969–1979, Jul. 2014.

[4] W. Lee, L. Xiang, R. Schober, and V. W. S. Wong, "Electric vehicle charging stations with renewable power generators: A game theoretical analysis," *IEEE Trans. Smart Grid*, vol. 6, no. 2, pp. 608–617, Mar. 2015.

[5] R. Couillet, S. M. Perlaza, H. Tembine, and M. Debbah, "Electrical vehicles in the smart grid: A mean field game analysis," *IEEE J. Sel. Areas Commun.,* vol. 30, no. 7, pp. 1086–1096, Jul. 2012.

[6] H. Yang *et al.*, "Electric vehicle route optimization considering time-of-use electricity price by learnable partheno-genetic algorithm," *IEEE Trans. Smart Grid,* vol. 6, no. 2, pp. 657–666, Mar. 2015.

[7] E. Yudovina and G. Michailidis, "Socially optimal charging strategies for electric vehicles," *IEEE Trans. Autom. Control*, vol. 60, no. 3, pp. 837–842, Mar. 2015.

[8] B. Geng, J. Mills, and D. Sun, "Two-stage charging strategy for plug-in electric vehicles at the residential transformer level," *IEEE Trans. Smart Grid*, vol. 4, no. 3, pp. 1442–1452, Sep. 2013.

[9] H. Sekyung, H. Soohee, and K. Sezaki, "Development of an optimal vehicle-to-grid aggregator for frequency regulation," *IEEE Trans. Smart Grid*, vol. 1, no. 1, pp. 65–72, Jun. 2010.

[10] J. Tan and L. Wang, "Integration of plug-in hybrid electric vehicles into residential distribution grid based on two-layer intelligent optimization," *IEEE Trans. Smart Grid,* vol. 5, no. 4, pp. 1774–1784, Jul. 2014.

[11] H. Nguyen and J. Song, "Optimal charging and discharging for multiple PHEVs with demand side management in vehicle-to-building," *J. Commun. Netw.*, vol. 14, no. 6, pp. 662–671, Dec. 2012.

[12] E. Sortomme, M. Hindi, and S. Macpherson, "Coordinated charging of plug-in hybrid electric vehicles to minimize distribution system losses," *IEEE Trans. Smart Grid*, vol. 2, no. 1, pp. 198–205, Mar. 2011.

[13] A. Kotsialos, M. Papageorgiou, C. Diakaki, Y. Pavlis, and F. Middelham, "Traffic flow modeling of large-scale motorway networks using the macroscopic modeling tool METANET," *IEEE Trans. Intell. Transp. Syst.*, vol. 3, no. 4, pp. 282–292, Dec. 2002.

[14] *National Household Travel Survey*. (2009). [Online]. Available: http://nhts.ornl.gov, accessed Mar. 18, 2015.

[15] A. Mohsenian-Rad, V. M. S. Wong, J. Jatskevichi, R. Schober, and A. Leon-Garcia, "Autonomous demand-side management based on game-theoretic energy consumption scheduling for the future smart grid," *IEEE Trans. Smart Grid,* vol. 1, no. 3, pp. 320–331, Dec. 2010.

[16] P. Samadi, A. Mohsenian-Rad, R. Schober, V. W. S. Wong, and J. Jatskevich, "Optimal real-time pricing algorithm based on utility maximization for smart grid," in *Proc. IEEE Conf. Smart Grid Commun.*, Gaithersburg, MD, USA, 2010, pp. 415–420.

[17] L. Chen, N. Li, S. H. Low, and J. C. Doyle, "Two market models for demand response in power networks," in *Proc. IEEE Conf. Smart Grid Commun.*, Gaithersburg, MD, USA, 2010, pp. 397–402.

[18] R. Nelson, *Probability, Stochastic Processes, and Queueing Theory*. New York, NY, USA: Springer, 1995.

[19] H. M. Taylor and S. Karlin, *An Introduction to Stochastic Modeling,* 3rd Ed. Orlando, FL, USA: Academic Press, 1998.

[20] J. He, Y. Sun, P. Wang, and L. Cheng, "A hybrid conditions-dependent outage model of transformer in reliability evaluation," *IEEE Trans. Power Del.*, vol. 24, no. 4, pp. 2025–2033, Oct. 2009.

[21] T. Vincent, *Evolutionary Game Theory, Natural Selection, and Darwinian Dynamics*, Cambridge. U.K.: Cambridge Univ. Press, 2005.

[22] J. B. Rosen, "Existence and uniqueness of equilibrium points for concave N-person games," *Econometrica,* vol. 33, no. 3, pp. 520–534, Jul. 1965.

[23] S. Hemon, M. Rougemont, and M. Santha, "Approximate Nash equilibria for multi-player games," in *Algorithmic Game Theory* (LNCS 4997). Berlin, Germany: Springer-Verlag, 2008, pp. 267–278.

[24] N. G. Pavlidis, K. E. Parsopoulos, and M. N. Vrahatis, "Computing Nash equilibria through computational intelligence methods," *J. Comput. Appl. Math.*, vol. 175, no. 1, pp. 113–136, Mar. 2005.

[25] J. Kennedy and R. C. Eberhart, "Particle swarm optimization," in *Proc. IEEE Conf. Neural Netw.,* Perth, WA, Australia, pp. 1942–1948.

[26] W. H. Kersting, "Radial distribution test feeders," in *Proc. IEEE PES Winter Meeting,* Columbus, OH, USA, 2001, pp. 908–912. [Online]. Available: http://ewh.ieee.org/soc/pes/dsacom/

[27] Z. Wang, R. Yang, L. Wang, and J. Tan, "Reliability assessment of integrated residential distribution and PHEV systems using Monte Carlo simulation," in *Proc. IEEE PES Gen. Meeting*, Vancouver, BC, Canada, 2013, pp. 1–5.

[28] R. Billinton and W. Li, *Reliability Assessment of Electric Power System Using Monte Carlo Methods.* New York, NY, USA: Plenum Press, 1994.

Jun Tan (S'13) received the B.S. and M.S. degrees in electrical engineering from the Huazhong University of Science and Technology, Wuhan, China, in 2009 and 2012, respectively. He is currently pursuing the Ph.D. degree in electrical engineering with the Department of Electrical Engineering and Computer Science, University of Wisconsin–Milwaukee (UWM), Milwaukee, WI, USA.

His current research interests include grid integration of electric vehicles, electric vehicles charging navigation, networked microgrids, power system analysis and operations, power system reliability assessment, and renewable energy integration.

Mr. Tan was a recipient of the Distinguished Graduate Student Fellowship Award from UWM.

Lingfeng Wang (S'02–M'09) received the B.E. degree in measurement and instrumentation from Zhejiang University, Hangzhou, China, in 1997; the M.S. degree in electrical and computer engineering from the National University of Singapore, Singapore, in 2002; and the Ph.D. degree from the Department of Electrical and Computer Engineering, Texas A&M University, College Station, TX, USA, in 2008.

He is currently an Associate Professor with the Department of Electrical Engineering and Computer Science, University of Wisconsin–Milwaukee, Milwaukee, WI, USA, where he directs the Cyber-Physical Energy Systems Research Group. He was an Assistant Professor with the University of Toledo, Toledo, OH, USA, and an Associate Transmission Planner with the California Independent System Operator, Folsom, CA, USA. His current research interests include power system reliability and resiliency, smart grid cybersecurity, renewable energy integration, intelligent and energy-efficient buildings, electric vehicles integration, microgrid analysis and management, and cyber-physical systems.

Prof. Wang is an Editor of the IEEE TRANSACTIONS ON SMART GRID and serves on the Steering Committee of the IEEE TRANSACTIONS ON CLOUD COMPUTING. He serves as the Co-Chair for the IEEE SmartGridComm'15 Symposium on Data Management, Grid Analytics, and Dynamic Pricing. He is an Editorial Board Member for several international journals, including *Sustainable Energy Technologies and Assessments* and *Intelligent Industrial Systems*.